

Influence of point defects on the metal-insulator transition in BaVS₃

Ana Akrap,^{1,*} Aurore Rudolf,² Florence Rullier-Albenque,³ Helmuth Berger,¹ and László Forró¹

¹*Institut de Physique de la Matière Complexe, EPFL, CH-1015 Lausanne, Switzerland*

²*Institut de Physique des Nanostructures, EPFL, CH-1015 Lausanne, Switzerland*

³*SPEC, Orme des Merisiers, CEA, 91191 Gif sur Yvette Cedex, France*

(Received 15 January 2008; revised manuscript received 5 March 2008; published 28 March 2008)

To investigate the nature of the metal-insulator transition which takes place in BaVS₃ at $T_{\text{MIT}}=70$ K, we study pure samples of BaVS₃ irradiated by fast electrons, which introduce point defects. Our results show that the metal-insulator transition is gradually weakened and shifted to lower temperatures by introducing the defects, in close analogy to systems where metal-insulator transition is due to a Peierls mechanism. Additionally, we study the influence of point defects on the temperature-pressure phase diagram of BaVS₃.

DOI: [10.1103/PhysRevB.77.115142](https://doi.org/10.1103/PhysRevB.77.115142)

PACS number(s): 71.30.+h, 72.10.Fk

I. INTRODUCTION

BaVS₃ is a quasi-one-dimensional itinerant spin-1/2 system, built from VS₃ chains spaced by barium atoms. The vanadium $3d^1$ electron is equally shared between two bands, a wide quasi-one-dimensional d_{z^2} and a narrow isotropic e_g band.^{1,2} Despite the chainlike crystal structure and the quasi-one-dimensionality, BaVS₃ is electrically nearly isotropic.³ It is believed that this is due to the fact that electron correlations strongly reduce the on-chain conductivity. At ambient pressure, the compound undergoes three transitions: a structural transition from hexagonal to orthorhombic symmetry at $T_S \approx 240$ K, a metal-insulator transition at $T_{\text{MI}} \approx 70$ K, and a magnetic transition at $T_X = 30$ K, where an incommensurate antiferromagnetic order is established. By diffuse x-ray scattering, it was observed that a commensurate tetramerized structure develops below T_{MI} , suggestive of a Peierls transition in the quasi-one-dimensional d_{z^2} band.⁴ However, no charge disproportionation larger than $0.01e^-$ was found below T_{MI} by anomalous scattering at vanadium K edge.⁵ Therefore, it is still not firmly established what is the mechanism of the metal-insulator (MI) transition. In many classical charge or spin density wave systems, it has been studied how the radiation damage influences the phase transition. A similar response of the metal-insulator transition in BaVS₃ to point defects may suggest that its origin is in the long-range density wave formation. Irradiation by a beam of fast electrons can be used to produce defects in a controlled way. Studies of several systems featuring a Peierls phase transition have shown that point defects locally perturb the coherency of the static charge ordering and may ultimately prevent the system from long-range ordering.

The presence of defects is also related to an interesting issue in BaVS₃: its extreme sensitivity to disorder, seen in several of its physical properties.⁶ For example, sulfur content has a very important influence on the properties of BaVS₃. Strongly sulfur-deficient samples are known to exhibit no MI transition and to have a ferromagnetic ground state.⁷ Moreover, the structural transition occurring at T_S can be detected in the resistivity only in the samples with a stoichiometric sulfur content. Still, no systematic study of how the defects influence the MI transition, and the phase diagram has been investigated so far.

Here, we report an ambient and high-pressure transport study of BaVS₃ where point defects were induced by fast electron irradiation. We find that by introducing interstitials and vacancies by knock-on collisions, the MI transition is progressively smeared out and shifted to lower temperatures. Under high pressure, the T_{MI} line in the phase diagram is pushed toward lower pressures.

II. METHODS

The crystals of BaVS₃ were grown in tellurium flux and annealed in sulfur atmosphere at high temperature.⁸ Several long needlelike crystals were cut perpendicular to the chain direction. In this study, we use six samples, coming from two single crystals. The starting crystals are of high quality, which is evidenced by a sharp metal-insulator transition at ambient pressure and a high residual resistivity ratio (~ 50) in the metallic phase, under 2.0 GPa. The samples obtained by cutting the starting crystals across the chain direction have typical dimensions of $1.25 \times 0.20 \times 0.20$ mm³. The irradiations are carried out with 2.5 MeV electrons in the low-temperature facility of the Van de Graaff accelerator at the LSI of Ecole Polytechnique in Palaiseau. Electron fluences ranging from 0.0 up to 6.65×10^{19} e⁻/cm² are applied to various pieces of the cut single crystals. The irradiation is performed with the samples immersed in liquid hydrogen at the temperature of 20 K. The electron flux is limited to 10^{14} e⁻/cm² s to avoid heating of the samples during irradiation. The thickness of the samples (~ 200 μ m) is small compared to the penetration depth of the electrons, warranting homogeneous damage throughout the samples. Ambient pressure resistivity is measured *in situ*, along the VS₃ chains. The susceptibility and magnetization are measured in a Quantum Design superconducting quantum interference device apparatus. The high-pressure resistivity measurements are performed in a clamped piston-cylinder cell, where kerosene is used as pressure medium.

III. RESULTS AND DISCUSSION

The top panel of Fig. 1 shows the temperature dependence of the resistivity for a single sample repetitively treated by electron radiation. The measurements of resistivity are per-

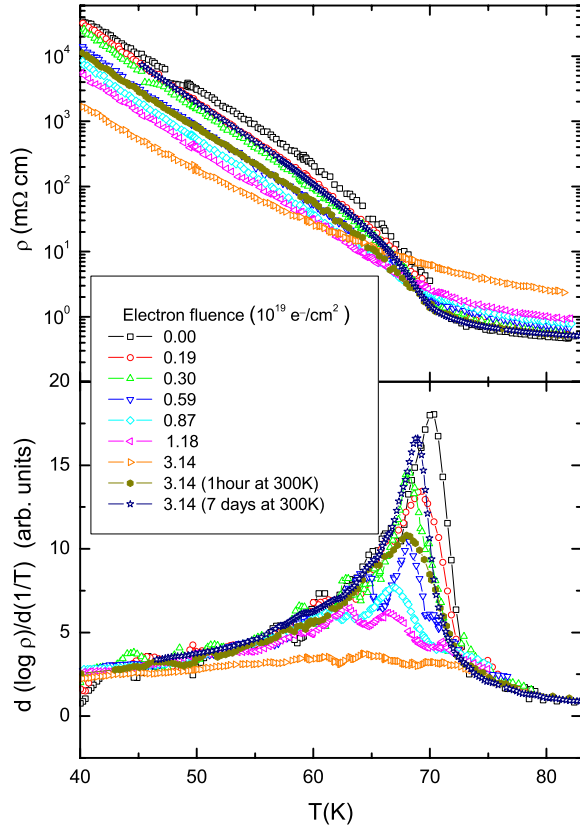


FIG. 1. (Color online) The temperature dependence of resistivity (top panel) and its logarithmic derivative for the same single crystal irradiated by different electron fluences. The sample was kept below 100 K, except in the case of the last two curves where the annealing time and temperature are indicated in the parentheses.

formed *in situ*, at ambient pressure, directly after irradiating the sample and annealing it for a brief interval of several minutes at 100 K. The defects produced by irradiation are fairly sensitive to thermal migration, which is why the temperature range of the measurement is limited to 20–80 K. The resistivity of the sample above the MI transition increases under irradiation. The lower panel of Fig. 1 shows the logarithmic derivative $d(\log \rho)/d(1/T)$ in the same temperature range. The transition at 70 K in the pure sample shifts to lower temperatures and is significantly widened by the presence of defects. In fact, before the T_{MI} is decreased by 10 K, the metal-insulator transition is already completely smeared out. The broadening and the shift of the transition under the influence of defects have been seen in several systems that undergo a charge-density wave (CDW) transition.⁹ Such behavior is reminiscent of a Peierls mechanism driving the metal-insulator transition. Because the defects pin the phase of the density wave, coherence between the chains is weakened. The transition is thus shifted to lower temperatures and gradually suppressed. The decrease in T_{MI} is monotonous and approximately linearly dependent on electron fluence, as can be seen in Fig. 2.

The resistivity at temperatures below the MI transition decreases as the electron dose is increased. After irradiating the sample by a fluence of $3.14 \times 10^{19} e^-/\text{cm}^2$, the resistivity

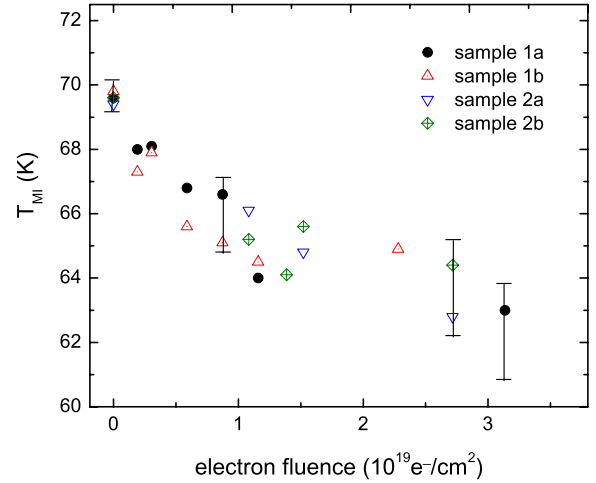


FIG. 2. (Color online) The dependence of the transition temperature on the electron fluence during the irradiation of four different samples. The samples were maintained on temperatures below 100 K.

at 35 K decreases by more than 20 times. There are two reasons for the lowered resistivity. First, the defects introduce localized states through which electrons can hop, enhancing the conductivity of the insulating phase. Second, the semiconducting gap is weakened because the pinning effect decreases the coherence volume of the CDWs. The value of the semiconducting gap decreases as the irradiation dose grows from the initial value of ~ 530 to ~ 440 K after the dose of $3.14 \times 10^{19} e^-/\text{cm}^2$. Here, the values of gap are extracted from the temperature dependence of the resistivity between 50 and 30 K using a fit to the activated behavior,

$$\rho = \rho_0 \exp \frac{\Delta}{k_B T}. \quad (1)$$

A similar disorder-induced decrease in the gap has previously been observed in several CDW systems.⁹

When the samples of BaVS_3 are irradiated by the flux of fast electrons at the temperature of 20 K, various scattering processes may take place, resulting in displacements in all the three atomic sublattices. The cross sections for Ba, V, and S atoms depend on the value of the threshold energy E_d , which is the minimum energy necessary to eject an atom from its site. Typical values of E_d range from 10 to 30 eV depending on the structure and material. For example, E_d values for O and Cu displacements in $\text{YBa}_2\text{Cu}_3\text{O}_{7-\delta}$ are, respectively, 10 and 15 eV.¹⁰ As BaVS_3 is a rather open structure, we may suppose that the values of E_d are relatively low. The number of defects created per VS_3 unit is $n_d = \sigma_d^i \phi t$, where σ_d^i is the cross section for displacing the atom i from its site and ϕt is the electron fluence. Calculations of n_d , by taking, for instance, $E_d = 5$ eV for S and 15 eV for V, lead to a total number of displaced V and S atoms per VS_3 plane $n_d = 2.0 \times 10^{-2}$ for an electron fluence of $10^{19} e^-/\text{cm}^2$. Here, we do not consider the defects in the Ba sublattice because E_d for Ba is presumably large, and moreover, these defects would not be expected to have such an important influence

onto the physics of BaVS_3 as S and V defects. Finally, even though this absolute value of n_d may not be very accurate, it allows a comparison between the different crystals studied.

Annealing the sample at room temperature drastically reduces the concentration of impurities. From a sample irradiated by $3.14 \times 10^{19} e^-/\text{cm}^2$, shown in Fig. 1, where the transition is practically wiped out, the annealing at 300 K for several days recovers the phase transition at a temperature with only a slightly less sharp peak in the logarithmic derivative and merely ~ 1 K lower than in the pure sample. This indicates that a vast part of the defects are easily recombined through thermal diffusion. The peak in the resistivity derivative of the $3.14 \times 10^{19} e^-/\text{cm}^2$ curve is positioned between the peaks of the curves measured *in situ* after irradiation fluences of $(0.19-0.3) \times 10^{19} e^-/\text{cm}^2$. Using the above estimates of displacement cross sections, this would correspond to $n_d \sim 5 \times 10^{-3}$, i.e., 0.5% V and S displacements per unit formula. Since the sulfur atoms are expected to thermally migrate easier than the vanadium atoms, when the sample is annealed by warming up to room temperature, it is likely that the majority of the remaining defects are in the V sublattice.

Another way of estimating the number of defects which remain after electron irradiation and a subsequent annealing at 300 K is through a measurement of magnetic susceptibility. We have investigated three pieces of the starting single crystal, irradiated, respectively, by the total electron fluences of 3.3×10^{19} , 1.6×10^{19} , and $0.0 e^-/\text{cm}^2$. The irradiated samples showed a decrease in the T_{MI} of 1.9 and 0.8 K, respectively. For a pure BaVS_3 sample, the temperature dependence of magnetic susceptibility shows a $1/T$ behavior down to T_{MI} , a sharp antiferromagneticlike drop below the MI transition, and a negligible Curie tail below ~ 15 K.³ The presence of defects does not significantly influence the high-temperature part, but it considerably increases the low-temperature Curie contribution. The magnitude of the Curie tail due to the presence of defects can be evaluated using the following formula:

$$\chi = \frac{N_{\text{def}} \mu_{\text{eff}}^2}{T}. \quad (2)$$

Here, N_{def} is the density of defects and μ_{eff} is their effective magnetic moment. If we assume that the majority of the defects in the samples are due to spin-1/2 cations V^{4+} and spin-1/2 anions S^- , we obtain that the effective spin-only moment is $\mu_{\text{eff}} \approx 1.73 \mu_B$. Using the above formula, we may estimate that the density of defects corresponding to a fluence of $10^{19} e^-/\text{cm}^2$ and a subsequent annealing at room temperature for several days approximately equal 0.5% of defects per unit formula. The latter result is approximately a factor of 3 of the estimate we got from the above calculation using the cross sections for V and S atom displacements, which implies that there may be other non-negligible contributions to the Curie tail.

As we have seen, the MI transition in BaVS_3 can be completely suppressed by introducing the point defects. Another way to do so is to apply hydrostatic pressure to the sample. The temperature dependence of the resistivity under various pressures, for a pristine sample and a sample with

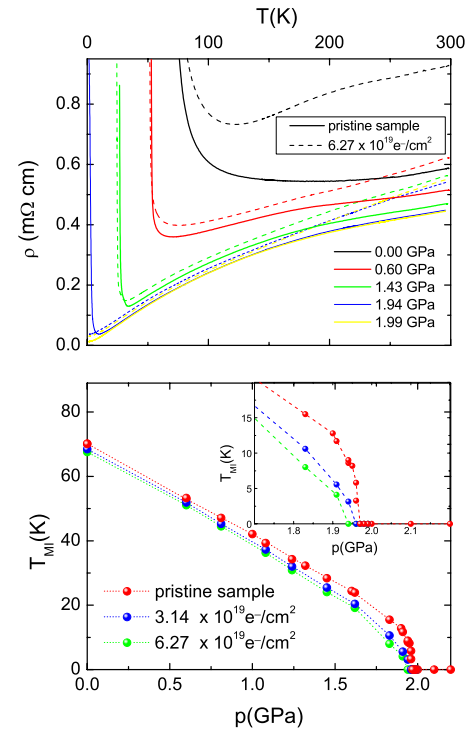


FIG. 3. (Color online) Top panel: temperature dependence of the resistivity at different pressures, shown for a pristine sample (straight line) and a sample irradiated by a fluence of $6.27 \times 10^{19} e^-/\text{cm}^2$. Bottom panel: phase diagram of a pristine sample of BaVS_3 , compared to two samples where defects were introduced by electron irradiation.

irradiation-produced point defects, is shown in the upper panel of Fig. 3. The external pressure gradually diminishes nesting, destroying the tetramerization along the chains, which leads to a decrease in T_{MI} and a complete suppression of the insulating phase under $p_{\text{cr}} \approx 2.0$ GPa.¹¹

The lower panel of Fig. 3 shows the phase diagram of BaVS_3 in the presence of defects, in comparison to a pure sample. We observe that the T_{MI} phase boundary is shifted to lower pressures and lower temperatures as the number of defects increases. The p_{cr} for a sample irradiated by $6.27 \times 10^{19} e^-/\text{cm}^2$ is 0.3 GPa lower than for the pristine sample. We believe that the reason there is a decrease in T_{MI} is the same as for the ambient pressure: adding the defects pins the phase of the CDW in the d_{z^2} band, which weakens the coherence between the chains. The semiconducting gap is related to the transition temperature through the mean field relation $\Delta = mk_B T_{\text{MI}}$. They are both determined by the energy gain which results from lowering the electronic state energy due to the lattice deformation. If the three-dimensional coherence volume of the CDWs is reduced by pinning effects on defects, the electronic energy gain is diminished and so is the Peierls gap. In case of BaVS_3 , $m \approx 12$ and seems to be approximately independent of pressure (up to ~ 1.8 GPa) (Ref. 12) and of defect concentration.

The most interesting part of the effect of point defects on the phase diagram is that close to p_{cr} . In the pristine sample, the insulating phase rapidly collapses above 1.7 GPa.¹³ This collapse is attributed to the strong interaction of the d_{z^2} and

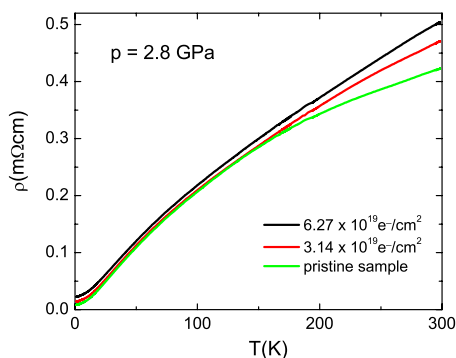


FIG. 4. (Color online) The temperature dependence of resistivity for three pieces of the same single crystal irradiated by different electron doses under 2.8 GPa.

e_g electrons. When pressure decreases the amplitude of the CDW, by reducing the nesting, the internal magnetic field generated by the e_g electrons further diminishes the nesting by the Zeeman splitting of $\pm k_F$. When point defects are present, they not only pin the CDW but also introduce disorder into the ferromagnetically arranged e_g electrons. The long-range magnetic order of the e_g electrons is then reduced and the collapse of the insulating phase becomes more gradual than for the pristine sample.

When $p \geq 2.0$ GPa, in a pure BaVS₃ sample, the Peierls transition is suppressed and a metallic state persists down to $T=0$ K. Figure 4 shows the resistivity curves for the three parts of a single crystal sample, irradiated by different electron fluences, under a high pressure, $p=2.8$ GPa. When defects are introduced into the sample, the resistivity is enhanced in the whole thermal range. Without dwelling on the details of the low-temperature dependence of resistivity, which will be discussed elsewhere,¹⁴ we focus on the high-temperature range. In particular, above ~ 150 K, the temperature dependence of the resistivity progressively becomes more linear as the defect density increases. A similar progression can also be seen in the resistivity curves at lower pressures (top panel of Fig. 3). Such an effect of defects on the

shape of the resistivity indicates that there may be a change in the energy dispersion of a collective mode responsible for the conduction electron scattering in this temperature range. Since at such high temperatures the electronic scale is expected to give less temperature dependence, a remaining possibility is that the introduced defects alter the phononic energy spectrum. For example, if point defects broaden the phonon dispersion, by modifying the elastic constants, then there may be more phonons available for electron-phonon scattering already at lower temperatures than in the pristine sample. This, in turn, lowers the temperature where a term linear in temperature appears in the resistivity. By Raman spectroscopy, two possible candidates were found, ~ 193 and ~ 350 cm^{-1} modes,¹⁵ which appear in the temperature range relatively close to room temperature. Finally, such a phononic interpretation of the high-temperature part of the resistivity is in accord with our rather elevated estimate of the defect density of the order of 1%.

IV. CONCLUSION

We have shown that the pinning of the density wave to the defects gradually destroys the three-dimensional order. With $\sim 5\%$ of defects, the metal-insulator transition is entirely suppressed. Furthermore, the influence of defects on the phase diagram is such that the T_{MI} is lowered and its sudden drop above 1.7 GPa becomes less pronounced. Finally, the strong influence of the defects on the thermal dependence of the resistivity at high temperature suggests that the point defects may infer changes to the phononic spectrum.

ACKNOWLEDGMENTS

We gratefully acknowledge discussions with Eduard Tutiš and Gørn Nilsen. It is a pleasure to thank Stephane Guillous from the van der Graaf accelerator of the Laboratoire des Solides Irradiés, Ecole Polytechnique in Palaiseau for the technical assistance. The work in Lausanne was supported by the Swiss National Science Foundation and its NCCR MaNEP.

*ana.akrap@epfl.ch

- ¹S. Mitrovic, P. Fazekas, C. Søndergaard, D. Ariosa, N. Barišić, H. Berger, D. Cloëta, L. Forró, H. Höchst, I. Kupčić, D. Pavnuna, and G. Margaritondo, *Phys. Rev. B* **75**, 153103 (2007).
- ²F. Lechermann, S. Biermann, and A. Georges, *Phys. Rev. B* **76**, 085101 (2007).
- ³G. Mihály, I. Kézsmárki, F. Zámorszky, M. Miljak, K. Penc, P. Fazekas, H. Berger, and L. Forró, *Phys. Rev. B* **61**, R7831 (2000).
- ⁴S. Fagot, P. Foury-Leylekian, S. Ravy, J.-P. Pouget, and H. Berger, *Phys. Rev. Lett.* **90**, 196401 (2003).
- ⁵S. Fagot, P. Foury-Leylekian, S. Ravy, J.-P. Pouget, É. Lorenzo, Y. Joly, M. Greenblatt, M. V. Lobanov, and G. Popov, *Phys. Rev. B* **73**, 033102 (2006).
- ⁶S. Fagot, P. Foury-Leylekian, J.-P. Pouget, G. Popov, M. Lobanov, M. Greenblatt, and P. Fertey, *Physica B* **378-380**, 1068 (2006).
- ⁷T. Yamasaki, H. Nakamura, and M. Shiga, *J. Phys. Soc. Jpn.* **69**,

3068 (2000).

- ⁸H. Kuriyaki, H. Berger, S. Nishioka, H. Kawakami, K. Hirakawa and F. A. Lévy, *Synth. Met.* **71**, 2049 (1995).
- ⁹L. Forró, A. Jánossy, L. Zuppiroli, and K. Bechgaard, *J. Phys. (Paris)* **43**, 977 (1982).
- ¹⁰A. Legris, F. Rullier-Albenque, E. Radeva, and P. Lejay, *J. Phys. I* **3**, 1605 (1993).
- ¹¹L. Forró, R. Gaál, H. Berger, P. Fazekas, K. Penc, I. Kézsmárki, and G. Mihály, *Phys. Rev. Lett.* **85**, 1938 (2000).
- ¹²I. Kézsmárki, G. Mihály, R. Gaál, N. Barišić, H. Berger, L. Forró, C. C. Homes, and L. Mihály, *Phys. Rev. B* **71**, 193103 (2005).
- ¹³N. Barišić, A. Akrap, H. Berger, and L. Forró, arXiv:0712.3395 (unpublished).
- ¹⁴A. Akrap, F. Rullier-Albenque, H. Berger, and L. Forró (unpublished).
- ¹⁵Z. V. Popović, G. Mihály, I. Kézsmárki, H. Berger, L. Forró, and V. V. Moshchalkov, *Phys. Rev. B* **65**, 132301 (2002).